



Brazilian Journal of Physics

ISSN: 0103-9733

luizno.bjp@gmail.com

Sociedade Brasileira de Física

Brasil

Güler, M.; Güler, E.

Theoretical Predictions for High-Pressure Elastic, Mechanical, and Phonon Properties of  
SiGe Alloy

Brazilian Journal of Physics, vol. 46, núm. 2, abril, 2016, pp. 192-197

Sociedade Brasileira de Física

São Paulo, Brasil

Available in: <http://www.redalyc.org/articulo.oa?id=46444888009>

- How to cite
- Complete issue
- More information about this article
- Journal's homepage in redalyc.org

redalyc.org

Scientific Information System

Network of Scientific Journals from Latin America, the Caribbean, Spain and Portugal

Non-profit academic project, developed under the open access initiative

# Theoretical Predictions for High-Pressure Elastic, Mechanical, and Phonon Properties of SiGe Alloy

M. Güler<sup>1</sup> · E. Güler<sup>1</sup>

Received: 30 September 2015 / Published online: 27 January 2016  
© Sociedade Brasileira de Física 2016

**Abstract** Elastic, mechanical, and phonon properties of zinc blende (ZB)-type SiGe ordered alloy were theoretically investigated in detail under pressures up to 12 GPa. Unlike earlier theoretical calculations of literature, a Stillinger-Weber-type interatomic potential was applied to this work for the first time with geometry optimization calculations. Pressure dependence of typical cubic elastic constants, bulk, shear and Young moduli, elastic wave velocities, Kleinman parameter, elastic anisotropy factor, phonon dispersion, as well as density of states of SiGe alloy were calculated and compared with other results when available. In general, our results for the above considered quantities of SiGe alloy are satisfactory and compare well the former theoretical data of alloy.

**Keywords** SiGe · Phonon · Elastic constants · Mechanical properties · GULP

**PACS Numbers** 61.66.Dk · 62.20.D- · 62.50.-p · 63.20.D-

## 1 Introduction

IV-IV semiconductor alloys (SiC, SiGe, GeC, SnC, and SiSn) have attracted much scientific and technological interest during the last few decades due to their superior physical and chemical properties.

Most significant properties of these alloys are high melting point, high thermal conductivity, large bulk modulus, large

band gap, and low dielectric constants [1]. Among them, SiGe alloys are still promising materials for modern electronic and optical devices [2], but they have received less attention when compared to SiC, GeC, and SnC alloys [1]. Apart from the limited experiments, various theoretical efforts have performed to clarify different physical properties of SiGe especially during the last decade [1, 3]. Qteish and Resta employed [4] norm-conserving pseudopotential scheme of density functional theory (DFT) to nine different ordered structures of  $\text{Si}_x\text{Ge}_{1-x}$  alloys and concluded that none of them was thermodynamically stable. In addition, Silva et al. [5] performed molecular dynamics (MD) calculations and found that  $\text{Si}_x\text{Ge}_{1-x}$  alloys crystallize at cubic structure at ambient conditions. Lv et al. [6] reported the high-pressure structural phase transitions of ordered  $\text{Si}_{50}\text{Ge}_{50}$  alloy with pseudopotential scheme of DFT and reported the phase transition pressure ( $P_T$ ) from zinc blende (ZB) phase to  $\beta$ -Sn phase as 12.3 GPa. Zhang et al. [1] also documented the structural, elastic, phononic, and temperature dependence of thermodynamic properties of SiSn, SiGe, and GeSn alloys in their DFT study. B. H. Elias [2] also applied plane-wave ultrasoft pseudopotential of DFT to his work for investigating the structural, elastic, optical, and thermodynamic properties of ordered SiSn, SiGe, and GeSn alloys.

Above recent and progressive theoretical attempts [5–9] on SiGe alloys inspired us to perform this work by addressing the high-pressure structural, elastic, mechanical, and other connected properties of SiGe alloy with a different method. Dissimilar to the theoretical methods used in literature [1, 2, 5–9], this work has been carried out by applying an existing Stillinger-Weber-type interatomic potential for the first time with geometry optimization calculations to clarify the mentioned quantities of SiGe alloy under pressures up to 12 GPa. The following part of the paper gives the details of our theoretical calculations with the employed interatomic potential and structure optimization in Sect. 2. We also confer our

✉ M. Güler  
mlkgnr@gmail.com

<sup>1</sup> Department of Physics, Hitit University, 19030 Corum, Turkey

results with the previous theoretical data through the results and discussion part of the paper in Sect. 3. Finally, Sect. 4 summarizes the main findings of this work in the conclusions.

## 2 Details of Theoretical Calculations

Although Stillinger-Weber (SW)-type interatomic potential was proposed almost 30 years ago, it is still in wide use nowadays. This unceasing interest originates from its success in modeling semiconductor materials involving silicon [9]. Therefore, we have applied SW-type potential of Laradji et al. [10] to this work which is originally designed to predict the structural properties of  $\text{Si}_x\text{Ge}_{1-x}$  alloys. Details about the applied potential and its parameterization procedure can be also in [10]. On the other hand, all theoretical calculations were carried out with the General Utility Lattice Program (GULP) 4.2. molecular dynamics code [11, 12]. This useful code allows optimizing the concerned structures at constant pressure (all internal and cell variables are included) or at constant volume (unit cell remains frozen). To avoid the constraints, constant pressure optimization was applied to the geometry of ZB-type SiGe cell with the Newton–Raphson method based on the Hessian matrix calculated from the second derivatives. The cell geometry of ZB-type SiGe was assigned similar to previous theoretical data of Zhang et al. [1] and Elias [2] with the lattice parameters  $a=b=c=5.47\text{\AA}$ ,  $\alpha=\beta=\gamma=90^\circ$  and space group  $F-43m$ . During present calculations, phonon and related properties of SiGe alloy were also addressed after constant pressure geometry optimization calculations as a function of pressure within the quasiharmonic approximation, at 0 K temperature, as implemented in GULP code. It is possible to obtain the phonon density of states (DOS) and dispersions for a given crystal after specifying a shrinking factor with GULP phonon calculations. As well, phonons are described by calculating their values at points in reciprocal space within the first Brillouin zone of the related crystal. To achieve the Brillouin zone integration and get the DOS, we have used a standard and reliable scheme developed by Monkhorst and Pack [13] with  $8 \times 8 \times 8$   $k$ -point mesh.

After setting the necessities for geometry optimization of ZB-type SiGe, we performed multiple runs at 0 K temperature and checked the pressure ranges between 0 and 12 GPa in the steps of 2 GPa. During our geometry optimization calculations, the Hessian matrix was recursively updated using the BFGS [14–17] algorithm.

## 3 Results and Discussion

$C_{11}$ ,  $C_{12}$ , and  $C_{44}$  are the typical cubic elastic constants which describe the mechanical hardness of a material and desirable for estimating the stability of regarding material. These elastic

constants derived from the total energy calculations represent the single crystal elastic properties. However, Voigt-Reuss-Hill average values yield confident results for the elastic constants of polycrystalline materials [18–22]. To get the precise values of typical cubic elastic constants and other related quantities of ZB SiGe, we considered the Voigt-Reuss-Hill values. Figure 1 outlines the pressure dependency of the  $C_{11}$ ,  $C_{12}$ , and  $C_{44}$  between the pressures 0 and 12 GPa. It is obvious from Fig. 2 that the calculated values of elastic constants  $C_{11}$ ,  $C_{12}$ , and  $C_{44}$  are positive where  $C_{11}$  and  $C_{12}$  have sharp increments as a function of increasing pressure. Further, the increment of the elastic constant  $C_{11}$  is higher than the both elastic constants  $C_{12}$  and  $C_{44}$ . From a physical outlook,  $C_{11}$  signifies the longitudinal elastic behavior, whereas  $C_{12}$  and  $C_{44}$  characterize the off diagonal and shear elastic characteristics of cubic crystals due to shearing, respectively. So, a longitudinal strain produces a change in volume without a change in shape. This volume change substantially related to pressure causes a larger change in  $C_{11}$ . Conversely, a transverse strain or shearing causes a change in shape without a change in volume. Therefore,  $C_{12}$  and  $C_{44}$  are less sensitive to pressure than  $C_{11}$ . Under zero pressure and temperature, our results for the pressure behavior and magnitudes of  $C_{11}$ ,  $C_{12}$ , and  $C_{44}$  are also compatible with the previous findings of Zhang et al. [1] and Elias [2] (see Table 1).

According to Born structural stability, the magnitudes of typical cubic elastic constants must obey the criteria  $C_{11}-C_{12}>0$ ,  $C_{11}>0$ ,  $C_{44}>0$ ,  $C_{11}+2C_{12}>0$  and cubic stability, i.e.,  $C_{12}>B>C_{11}$  condition [18–22]. As another result, calculated values of  $C_{11}$ ,  $C_{12}$ , and  $C_{44}$  elastic constants of ZB SiGe satisfy both the structural and cubic stability conditions, meaning that the crystal structure of ZB SiGe is stable under zero pressure and temperature. These results on both structural and cubic stability of ZB SiGe at ambient pressure and temperature are in well agreement with the results of Zhang et al. [1] and Elias [2].

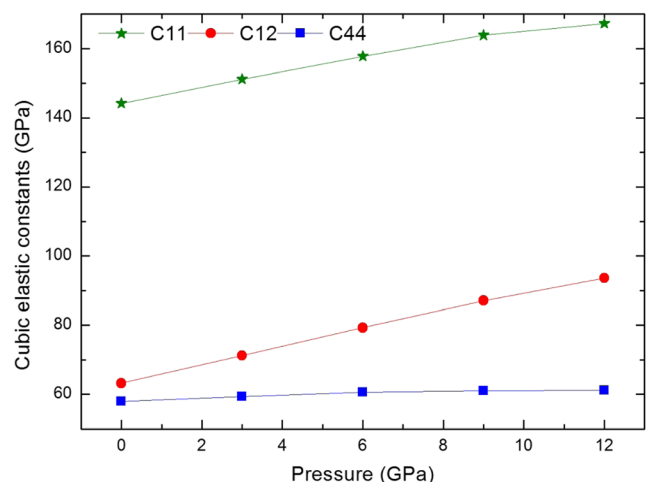
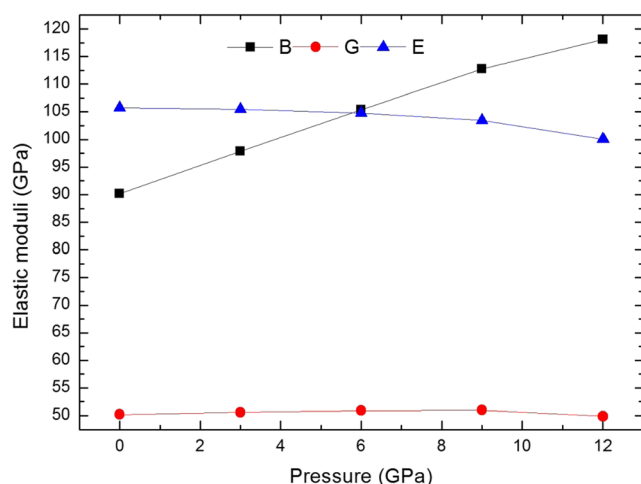


Fig. 1 Typical cubic elastic constants of ZB SiGe under pressure



**Fig. 2** Pressure dependence of bulk, shear, and Young moduli of ZB SiGe

Figure 2 displays the pressure behavior of bulk modulus ( $B$ ), shear modulus ( $G$ ), and Young modulus ( $E$ ) of ZB SiGe for the studied pressure range. These three elastic moduli ( $B$ ,  $G$ , and  $E$ ) are fundamental parameters necessary for controlling the mechanical properties of materials [18–22]. Among them, bulk modulus ( $B$ ) is the only elastic modulus of a material that delivers much knowledge about the bonding strength. It is also a measure of the material resistance to external deformation and expressed in many formulas explaining the diverse mechanical–physical properties [18–22]. The shear modulus ( $G$ ), however, defines the resistance to shape change caused by a shearing force and Young’s modulus ( $E$ ) is the resistance to uniaxial tensions. From the general physical definition of bulk modulus with  $B = \Delta P / \Delta V$ , one can expect an increment for  $B$  because of its direct proportion to the applied pressure. In Fig. 2, bulk modulus of ZB SiGe demonstrates uniform increment up to 12 GPa as expected.

**Table 1** Comparing the present results of some elastic and mechanical parameters of ZB SiGe alloy under zero pressure and temperature with former theoretical data

| Parameter                   | Present | Other theoretical results       |
|-----------------------------|---------|---------------------------------|
| $a$ (Å)                     | 5.47    | 5.46 [1], 5.45 [2]              |
| $C_{11}$ (GPa)              | 144.2   | 150.2 [1], 150.6 [2], 130.6 [7] |
| $C_{12}$ (GPa)              | 63.2    | 57.8 [1], 57.8 [2], 46.1 [7]    |
| $C_{44}$ (GPa)              | 57.9    | 75 [1], 74.9 [2], 67.8 [7]      |
| $B$ (GPa)                   | 90.2    | 88.6 [1], 87.6 [2], 74.3 [7]    |
| $G$ (GPa)                   | 50.2    | 61.7 [1], 56.1 [7]              |
| $E$ (GPa)                   | 105.7   | 150.3 [1], 118.5 [2], 134.5 [7] |
| $\nu$                       | 0.30    | 0.21 [1], 0.27 [2], 0.20 [7]    |
| $V_L$ (km s <sup>-1</sup> ) | 6.31    | 5.98 [7]                        |
| $V_S$ (km s <sup>-1</sup> ) | 3.56    | 3.67 [7]                        |
| $\zeta$                     | 0.57    |                                 |
| $A$                         | 1.42    | 1.62 [1], 1.61 [2], 1.60 [7]    |

Ductility and brittleness play key roles during materials manufacturing. Hence, we also appraised the ductile (brittle) characteristic of ZB SiGe crystal under pressure. The adjectives brittle and ductile indicate the two separate mechanical characteristics of solids when they subjected to external stress. In general, brittle materials are not deformable or less deformable before fracture. Oppositely, ductile materials are deformable a lot before fracture. For a separation, Pugh ratio is a determinative limit for ductile (brittle) behavior of materials and has a popular use in literature. If the  $B/G$  ratio of a material is about 1.75 and higher, the material is ductile; otherwise, the material becomes brittle [18–22]. Another reliable assessment criterion for ductility and brittleness is Cauchy pressure, which is expressed with  $C_P = C_{12} - C_{44}$ . The negative (positive) values of the Cauchy pressure reflect the brittle (ductile) nature of the related material [18–22]. Thus, we cross-checked our results with Pugh ratio and Cauchy pressure norms. Under zero pressure and temperature, our calculated numerical value for  $B/G$  is 1.8 and has a positive Cauchy pressure, which reveals the ductile nature of ZB SiGe crystal in contrast to the brittle verdict of Zhang et al. [1]. Moreover, in Fig. 3,  $B/G$  ratio has a linear increment under pressure and reaches its maximum value at 12 GPa.

Poisson ratio ( $\nu$ ) is the ratio between the transverse strain and longitudinal strain in the elastic loading direction. It can provide details about the bonding force behavior in solids [18–22]. The values of  $\nu = 0.25$  and  $\nu = 0.5$  portray the lower and upper limits of central forces, respectively. The present  $\nu$  value for ZB SiGe with 0.30 under zero pressure and temperature suggests that interatomic forces in ZB SiGe crystals are mainly central forces. This value for  $\nu$  (0.30) also agrees well the former theoretical result of Elias [2] with 0.27 and exhibits an increment tendency under pressure as in Fig. 4.

Low-temperature acoustic modes produce the vibrational excitations in solids. Due to these vibrations, two typical (longitudinal wave and shear wave) elastic waves arise [18–22] in materials. The velocities  $V_L$  and  $V_S$  symbolize longitudinal

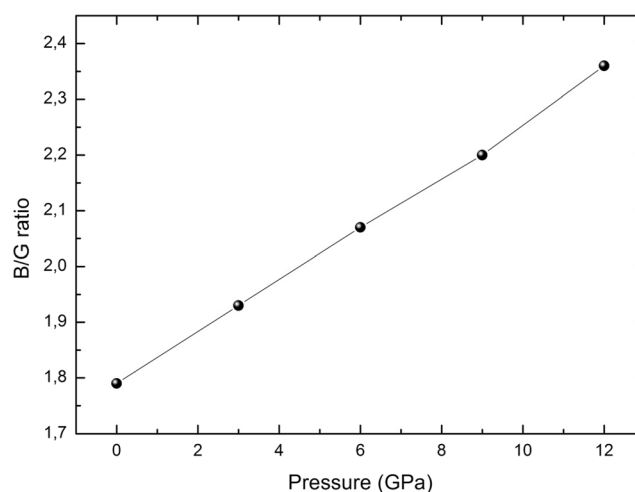


**Fig. 3**  $B/G$  ratio behavior of ZB SiGe under pressure

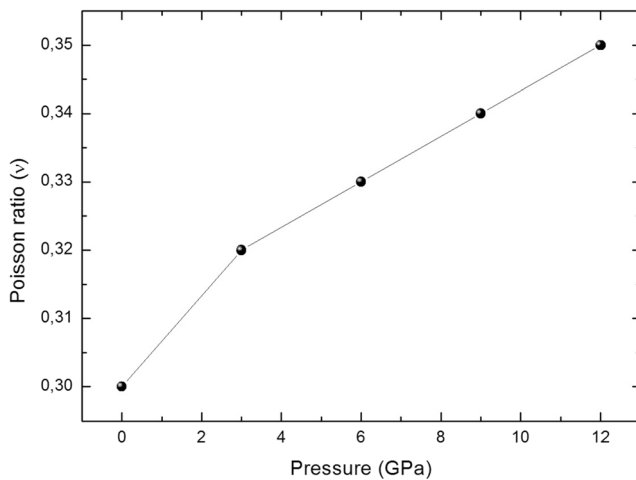


**Fig. 4** Pressure dependence of Poisson ratio of ZB SiGe

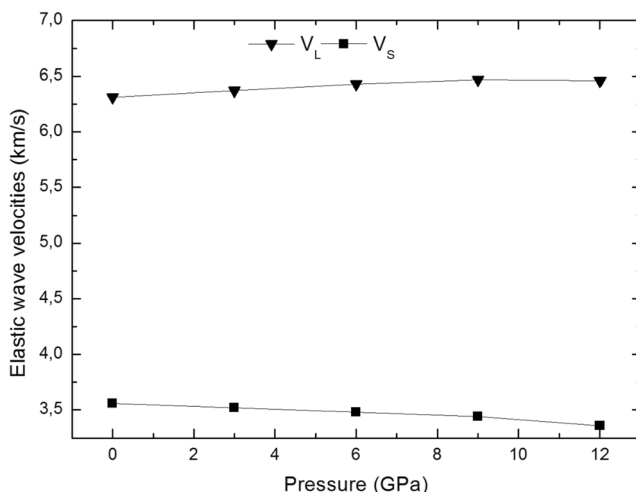
and shear wave velocities, respectively. Table 1 lists presently calculated numerical values of both velocities, and Fig. 5 illustrates the pressure behavior of  $V_L$  and  $V_S$  of ZB SiGe alloy. As in Fig. 5,  $V_L$  displays a gradual increment, whereas  $V_S$  has a sluggish decrease under pressure.

Kleinman parameter ( $\zeta$ ) describes the relative ease of bond bending to the bond stretching in cubic materials. Minimizing bond bending leads to  $\zeta=0$  and minimizing bond stretching leads to  $\zeta=1$  [18–22] and  $\zeta$  links to typical cubic elastic constants [23] as follows:

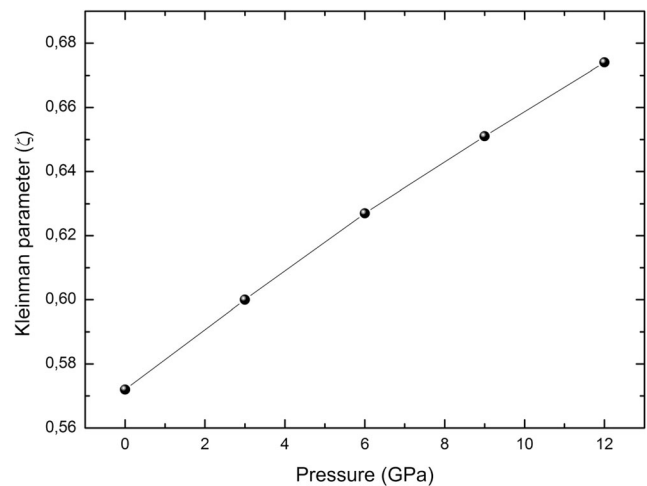
$$\zeta = (C_{11} + 8C_{12}) / (7C_{11} + 2C_{12})$$

Figure 6 displays the Kleinman parameter of ZB SiGe alloy upon the pressure increment. Under pressure,  $\zeta$  increases with increasing pressure. Our calculated numerical value for  $\zeta$  is 0.57 and reveals the bond stretching trend in ZB SiGe alloy under zero pressure and temperature.

The elastic anisotropy of crystals is crucial for engineering applications due to its strict correlation with the possibility of



**Fig. 5** Elastic wave velocities ( $V_L$  and  $V_S$ ) of ZB SiGe versus pressure



**Fig. 6** Behavior of Kleinman parameter of ZB SiGe under pressure

producing microcracks in materials. So, we also computed the elastic anisotropy factor:  $A = 2C_{44} / (C_{11} - C_{12})$  [24] to understand the elastic behavior of ZB SiGe. For an isotropic crystal, ( $A$ ) is the unity and any deviation from the unity gives the amount of elastic anisotropy [24]. Figure 7 demonstrates the elastic anisotropy factor of ZB SiGe alloy versus to applied pressure. The values of ( $A$ ) take place between 1.42 and 1.65 in the studied pressure range, which indicates the significant presence of elastic anisotropy in ZB SiGe alloy supporting the results of Zhang et al. [1] and Elias [2].

By computing the dynamical matrix in GULP package, the phonon dispersion of SiGe alloy is predicted for the chosen  $\Gamma$ -K high symmetry points and shown in Fig. 8. A closer look at the phonon dispersions in Fig. 8 shows the comparison between phonon dispersion computed from presently applied SW potential and the previous DFT data of Zhang et al. [1]. The circles display the previously obtained DFT data of SiGe whereas dashed lines represent our results for zero pressure and temperature phonon dispersions, respectively. It is evident from Fig. 8 that the low-frequency acoustic phonon

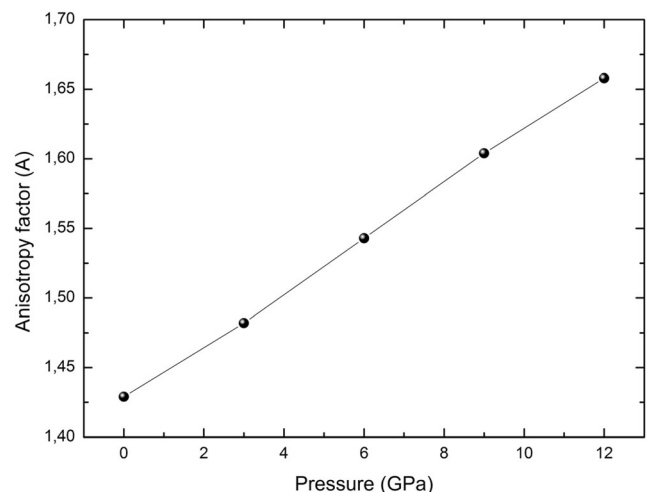


**Fig. 7** Elastic anisotropy parameter of ZB SiGe against to pressure

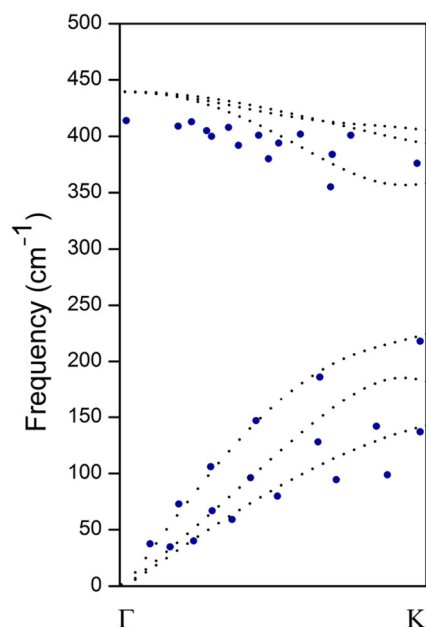


**Fig. 8** Phonon dispersion of ZB SiGe between the chosen  $\Gamma$  and K high symmetry points under zero pressure and temperature. The *circles* display the previously obtained DFT data [1], whereas *dashed lines* represent our results with the applied SW potential

modes of SiGe are well reproduced with applied potential while high-frequency optical-phonon modes are generally overestimated. Additionally, Fig. 9 displays the our results of both partial and total density of states for SiGe alloy under zero pressure and temperature. It is easy to see from Fig. 10 that both alloying elements (Si and Ge) contribute to the acoustic and optical modes. However, the contribution of Si is dominant for optical modes where Ge contribution is dominant for the acoustic modes. These results of alloying element contributions to the DOS of SiGe alloy well compare the DFT findings of Zhang et al. [1]. Further, there is an obvious gap in DOS curve between the frequencies 265 and

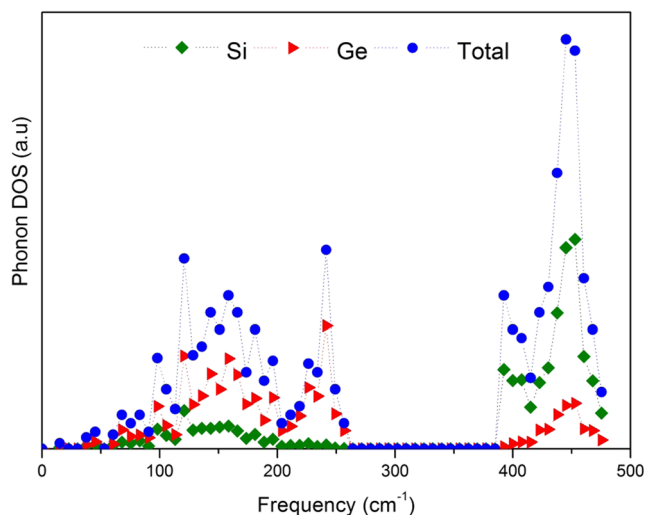


**Fig. 9** Partial and total density of states of ZB SiGe under zero pressure and temperature

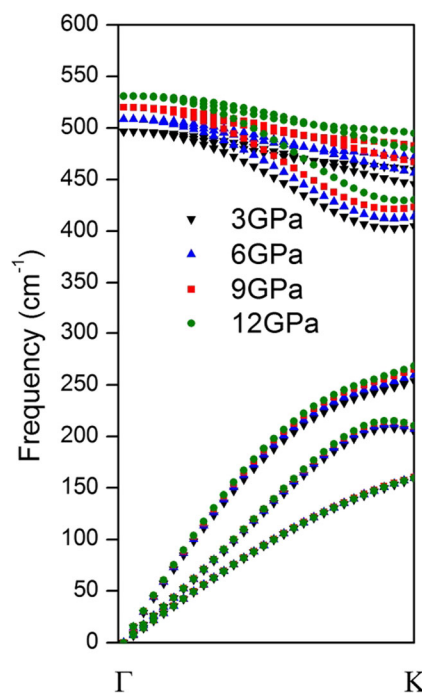


**Fig. 10** Phonon dispersion curve of ZB SiGe between the chosen  $\Gamma$  and K high symmetry points for 3, 6, 9, and 12 GPa pressures under zero temperature

$385 \text{ cm}^{-1}$  originating from the different masses of two alloying elements (Si and Ge). Our frequency values of DOS are comparable to DFT data of Zhang et al. [1] with the frequencies of 250 and  $330 \text{ cm}^{-1}$ .

Figure 10 shows the effect of pressure on the phonon dispersion and DOS of SiGe alloy along  $\Gamma$ -K region under pressures with 3, 6, 9, and 12 GPa. As seen in Fig. 10, both acoustic and optical phonon modes go toward to the higher frequency values under pressure and corresponding DOS peaks shift to higher frequencies (Fig. 11) as expected due to atoms which are getting closer to each other under pressure.

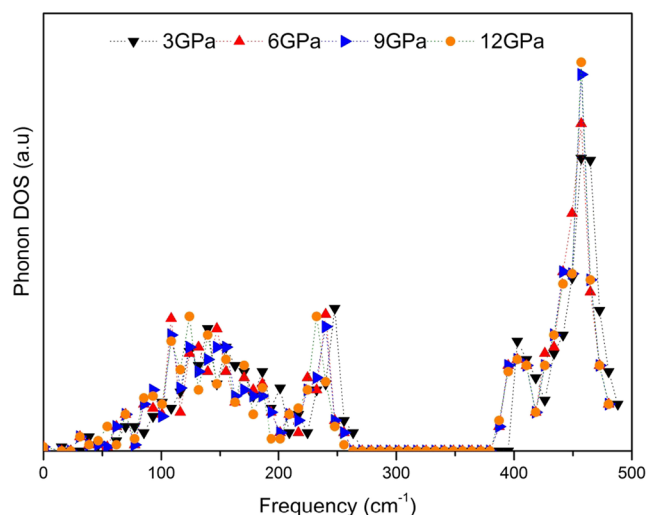


**Fig. 11** Total density of states of ZB SiGe SiGe under 3, 6, 9, and 12 GPa pressure and zero temperature



## 4 Conclusion

In summary, a different theoretical calculation was reported by employing an existing SW-type interatomic potential for the first time to elaborate the elastic, mechanical, and phonon behavior of ZB SiGe alloy under pressure. Presently, applied potential significantly reproduces well the high-pressure elastic, mechanical and low portion phonon modes of the alloy. Unfortunately, because of lack of experimental data, we compared our results only with available theoretical data. Presently obtained, typical cubic elastic constants, phonon dispersions and other obtained quantities under zero pressure and temperature are in good agreement with those of early theoretical data. Finally, our reasonable results may be further helpful to both experimental and theoretical works regarding the pressure dependence elastic and relevant properties of technologically important SiGe alloys.

## References

1. X. Zhang et al., *Superlattice Microst.* **52**, 459–469 (2012)
2. B.H. Elias, *Adv. Phys. Theor. Appl.* **25**, 82–91 (2013)
3. D.J. Paul, *Semicond. Sci. Technol.* **19**, R75 (2004)
4. A. Qteish, R. Resta, *Phys. Rev B* **37**, 1038 (1998)
5. C.R.S. da Silva et al., *Solid State Commun.* **120**, 369 (2001)
6. M.Y. Lv et al., *Solid State Commun.* **135**, 749 (2005)
7. A. Hao et al., *Phys. Status Solidi B* **248**(5), 1135–1138 (2011)
8. G. Grochola et al., *Chem. Phys. Lett.* **493**, 57–60 (2010)
9. L. Pizzagalli et al., *J. Phys.: Condens. Matter* **25**, 055801 (2001)
10. M. Laradji et al., *Phys. Rev. B* **51**(8), 4894–4901 (1995)
11. J.D. Gale, *Journal of the Chemical Society. Faraday Transactions* **93**(4), 629–637 (1997)
12. J.D. Gale, A.L. Rohl, *Molecular Simulation* **29**(5), 291–341 (2003)
13. H.J. Monkhorst, J.D. Pack, *Phys. Rev* **B13**, 5188 (1976)
14. C.G. Broyden, *J. Inst. Math. Appl.* **6**, 76 (1970)
15. R. Fletcher, *Comput. J.* **13**, 317 (1970)
16. D. Goldfarb, *Math. Comput.* **24**, 23 (1970)
17. D.F. Shanno, *Math. Comput.* **24**, 647 (1970)
18. E. Güler, M. Güler, *Mater. Res.* **17**, 1268–1272 (2014)
19. M. Güler, E. Güler, *J. Optoelectron, Adv. Mater.* **16**, 1222–1227 (2014)
20. E. Güler, M. Güler, *Chin. J. Phys.* **53**, 040807 (2015)
21. E. Güler, M. Güler, *Braz. J. Phys.* **45**, 296–301 (2015)
22. E. Güler and M. Güler, *Adv. Mater. Sci. Eng.*, Article ID 525673, 5 pages, (2013)
23. W.A. Harrison, *Electronic Structure and the Properties of Solids* (Dover Publications Inc, New York, 1980)
24. M. Ahmad et al., *J. Magn. Magn. Mater.* **377**, 204–210 (2015)